Competition between energy and phase relaxation in electronic curve crossing processes

John M. Jean and Graham R. Fleming

Citation: The Journal of Chemical Physics **103**, 2092 (1995); doi: 10.1063/1.469684
View online: http://dx.doi.org/10.1063/1.469684
View Table of Contents: http://scitation.aip.org/content/aip/journal/jcp/103/6?ver=pdfcov
Published by the AIP Publishing

Competition between energy and phase relaxation in electronic curve crossing processes

John M. Jean
Department of Chemistry, Washington University, St. Louis, Missouri 63130

Graham R. Fleming
Department of Chemistry and The James Franck Institute, University of Chicago, Chicago, Illinois 60637

(Received 17 January 1995; accepted 3 May 1995)

We present results from simulations of vibrational energy and phase relaxation and electronic curve crossing using a multilevel formulation of Redfield theory, which demonstrate the shortcomings of the optical Bloch approximation and the importance of coherence transfer processes in the relaxation dynamics of multilevel systems. Specifically, we show that for a harmonic well, energy relaxation can occur with retention of vibrational phase, and that for sufficiently strong electronic coupling, the product of an electronic curve crossing process can be formed vibrationally coherent even when no coherence is present in the initially excited state. © *1995 American Institute of Physics.*

I. INTRODUCTION

Improvements in femtosecond lasers have made the observation of vibrational quantum beats commonplace. Particular interest has been excited by the detection of oscillations in the stimulated emission[1] and spontaneous emission[2] of the special pair of the bacterial reaction center, and by the observation of oscillations in the transient absorption spectrum of the initial photoproduct of the retinal chromophore in the rhodopsin system.[3] These results imply that the two fundamental photobiological processes of photosynthesis and vision have initial steps that are fast compared to vibrational dephasing and thus have been referred to as ''coherent.'' Several other studies have observed coherent vibrational motion following what would generally be considered a curve crossing process. For example, Scherer *et al.*[4] see well-defined wave packet motion out to about 4 Å bond length following solvent-induced photodissociation of iodine from the bound B state to the dissociative a or a' states in hexane solution. Wynne *et al.*[5] find vibrational quantum beats produced in the ground state of the TCNE-HMB complex following optical excitation to the charge transfer state and subsequent intramolecular electron transfer back to the neutral state. Equally intriguing is the comparison of classical simulations and experimental studies of iodine caging in solid krypton described by Zadoyan *et al.*[6] Following excitation into the A state, very rapid energy relaxation occurs with significant retention of vibrational phase. Indeed at low temperature, vibrational phase is even partly retained for times up to 4 ps in iodine molecules reformed as a result of rebounding from the krypton cage.

These studies raise many challenges to conventional descriptions of vibrational and electronic relaxation based on the approximations of the optical Bloch equations. For a two-level system, the total dephasing rate in the optical Bloch picture is given by

$$\frac{1}{T_2}=\frac{1}{2}\left(\frac{1}{T_{1a}}+\frac{1}{T_{1b}}\right)+\frac{1}{T_2^*} \tag{1a}$$

or

$$\frac{1}{T_2}=\frac{1}{2T_1}+\frac{1}{T_2^*} \tag{1b}$$

depending on whether the lower level is infinitely long-lived or not. Here T_{1a} and T_{1b} are the population lifetimes of levels a and b and T_2^* is the pure dephasing time. In the second case, T_1 is the lifetime of the upper level. Thus T_2 can never exceed $2T_1$ or

$$T_2 \leqslant \frac{2T_{1a}T_{1b}}{T_{1a}+T_{1b}}. \tag{1c}$$

In the latter case, T_2 cannot exceed T_1 if $T_{1a}=T_{1b}=T_1$. Thus the observation of vibrational quantum beats has generally been taken to imply that vibrational energy relaxation is slow. Is this generally so or do relaxation pathways neglected at the optical Bloch level, i.e., coherence transfer terms, play an important role?

A second and related question raised by the experiments is: Can vibrational coherence be created in a reactive event (e.g., curve crossing) even if the initial state has little or no vibrational coherence or does such an observation imply a coherently vibrating reactant? Is optical excitation of a state different from preparation of the same state via an intermediate state? Further, can a nonadiabatic process lead to coherence in the product or does this require that the process proceed on a single electronic surface? If strong electronic coupling is required for coherence to be created in the product, are electronic recurrences expected in addition to the vibrational beats? Finally, if a vibrational wave packet is observed in the reactant but not in the product, does this mean that the coherent motion is not important in the reaction?

We have attempted to provide answers to these questions by means of simulations based on Redfield relaxation theory.[7–9] As described in more detail below, the ability to set particular elements of the Redfield tensor to zero allows a precise analysis of the applicability of the Bloch model to multilevel systems and the competition between vibrational and electronic relaxation and dephasing.

 0021-9606/95/103(6)/2092/10/$6.00

In the Redfield approach, the dynamics of a few ''system'' degrees of freedom are treated explicitly, while the remaining degrees of freedom comprise a thermal bath, which is weakly coupled to the system. A second order perturbative treatment of the system–bath coupling yields dissipative terms that correspond to transitions between system levels (population relaxation), random fluctuations of system energy levels (pure dephasing), coupling between populations and coherences, and transfer of coherences between pairs of levels. The latter two terms are neglected in the standard Bloch approximation.

Two model systems are considered here; (1) relaxation within a single harmonic surface and (2) electronic relaxation between two diabatic states following either optical or thermal preparation of one of the two states. We consider only a single vibrational degree of freedom; however, extension to multidimensional systems is straightforward.

II. REDFIELD FORMALISM

The elements of the reduced density matrix for the system obey the coupled Redfield equations[7]

$$\dot{\rho}_{ij}(t) = -i\omega_{ij}\rho_{ij} - \sum_{kl} R_{ij,kl}\rho_{kl}(t). \tag{2}$$

The first term on the right-hand side describes the free (coherent motion) of the system under the influence of its Hamiltonian. The second term corresponds to the dissipative effect of the environment on the system. Elements of the Redfield tensor, $R_{ij,kl}$, connect density matrix element ρ_{kl} at time t to element ρ_{ij} at some later time t'. A second-order treatment of the system–bath interaction yields the following expression for the tensor elements in terms of correlation functions of the system–bath coupling matrix elements:

$$\begin{aligned} R_{ij,kl} = -\frac{1}{\hbar^2}\int_0^\infty d\tau \Big[& \langle V_{lj}(0)V_{ik}(\tau)\rangle e^{-i\omega_{lj}\tau} \\ & + \langle V_{lj}(\tau)V_{ik}(0)\rangle e^{-i\omega_{ik}\tau} \\ & - \delta_{lj}\sum_s \langle V_{is}(\tau)V_{sk}(0)\rangle e^{-i\omega_{sk}\tau} \\ & - \delta_{ki}\sum_s \langle V_{ls}(0)V_{sj}(\tau)\rangle e^{-i\omega_{ls}\tau} \Big]. \end{aligned} \tag{3}$$

The Redfield equations are based on the assumption that the timescale of interest, Δt, is short compared to the relaxation times but long compared to the bath correlation time, τ_c. That is $R_{ij,kl}^{-1} > \Delta t > \tau_c$.

Elements of R in which the frequency mismatch $(\Delta\omega) = \omega_l - \omega_k - \omega_i + \omega_j = 0$ (i.e., secular terms) are particularly effective in the relaxation process. These include terms such $R_{ii,jj}$, $R_{ij,ij}$, and $R_{ij,kl}$ for which $\Delta\omega = 0$. The first two terms are rate constants for population transfer from state j to state i and dephasing of coherence between states i and j and are the analogs of the inverse T_1 and T_2 times in the simple Bloch model. The terms $R_{ij,kl}$ transfer coherence between states k and l to states i and j and have no analog in the Bloch model.

Nonsecular terms ($\Delta\omega \neq 0$) tend to be relatively ineffective in the relaxation process since their effect averages out for times, τ, that satisfy $\Delta\omega \cdot \tau > 1$. These include terms such as $R_{ii,ij}$, which couples populations and coherences and $R_{ij,kl}(\Delta\omega \neq 0)$, which connects coherences having different unperturbed time dependence. Walsh and Coalson[10] have recently carried out Redfield calculations on a harmonic oscillator linearly coupled to a harmonic bath that show that the importance of nonsecular terms on the relaxation dynamics increases as the system–bath interaction increases. In what follows, we keep both secular and nonsecular terms in the Redfield tensor.

The solution to the coupled Redfield equations can be expressed in the form

$$\rho(t) = e^{Lt}\rho(0), \tag{4}$$

where $\rho(0)$ denotes the density matrix at $t = 0$ and the L matrix is given by

$$L_{ij,kl} = -i\omega_{ij}\delta_{ik}\delta_{lj} - R_{ij,kl}. \tag{5}$$

Exact evaluation of the propagator, e^{Lt}, can be carried out via diagonalization of the L matrix as described in Ref. 8.

III. QUANTUM HARMONIC OSCILLATOR COUPLED TO A THERMAL BATH

In this section we discuss the structure of the Redfield relaxation tensor and compare results from simulations of relaxation of a harmonic oscillator obtained using the full Redfield tensor with those obtained from a multilevel Bloch model (i.e., only population relaxation and pure dephasing present). At issue are (1) Does the Bloch relation hold for the overall energy relaxation time, τ_E, and the coordinate damping time, τ_Q? (2) What effect do coherence transfer terms have on the relation between these two times? and (3) Does the Bloch relation hold for a pair of levels in a multilevel system?

We will denote the system coordinate as Q and the bath coordinates as $\mathbf{q}$. The coupling to the bath contains terms that are linear and quadratic in the system coordinate, $Q = (1/\sqrt{2})(a + a^+)$. The Hamiltonian is

$$H = H_S + H_B + V, \tag{6}$$

where

$$H_S = \left(a^+ a + \frac{1}{2}\right)\hbar\omega,$$

$$V = \frac{1}{\sqrt{2}} f_1(\mathbf{q})(a + a^+) + \frac{1}{2} f_2(\mathbf{q})(a + a^+)^2,$$

and a^+ and a are the boson creation and annihilation operators. The linear coupling term connects states that differ by one quantum of energy and are thus give rise to one-phonon

relaxation processes. The quadratic term introduces pure dephasing into our model in addition to two-phonon relaxation processes.

Examples of the secular terms that arise from this form of the system–bath coupling are shown below;
one-phonon relaxation $(j\rightarrow i)$,

$$R_{ii,jj}=\frac{-1}{\hbar^2}\,|\langle i|Q|j\rangle|^2[J_1^-(\omega_{ji})+J_1^+(\omega_{ij})] \qquad |j-i|=1, \tag{7a}$$

two-phonon relaxation $(j\rightarrow i)$,

$$R_{ii,jj}=\frac{-1}{\hbar^2}\,|\langle i|Q^2|j\rangle|^2[J_2^-(\omega_{ji})+J_2^+(\omega_{ij})] \qquad |j-i|=2, \tag{7b}$$

population decay of level i,

$$R_{ii,ii}=\frac{1}{T_{1,i}}=\sum_{s\neq i}R_{ss,ii} \qquad |s-i|=1,2, \tag{7c}$$

dephasing,

$$R_{ij,ij}=\frac{1}{T_2}=\frac{1}{\hbar^2}\,(\langle i|Q^2|i\rangle-\langle j|Q^2|j\rangle)^2[J_2(0)] \quad \text{(pure dephasing)} + \frac{1}{2}\left(\sum_{s\neq i}R_{ss,ii}+\sum_{s\neq i}R_{ss,jj}\right) \qquad |j-i|=0,1,2, \tag{7d}$$

coherence transfer (one-phonon terms),

$$R_{ij,jk}=\frac{-1}{\hbar^2}\,\langle k|Q|j\rangle\langle i|Q|j\rangle[J_1^-(\omega_{kj})+J_1^+(\omega_{ij})] \qquad |k-i|=2 \qquad |l-j|=2, \tag{7e}$$

coherence transfer (two-phonon terms),

$$R_{ij,kl}=\frac{-1}{\hbar^2}\,\langle l|Q^2|j\rangle\langle i|Q^2|k\rangle[J_2^-(\omega_{lj})+J_2^+(\omega_{ik})] \qquad |l-j|=2 \qquad |k-j|=2. \tag{7f}$$

The spectral densities, $J_i(\omega)$, are given by

$$J_i^+(\omega_{ij})=\int_0^\infty d\tau\langle f_i(q,\tau)f_i(q,0)\rangle e^{-i\omega_{ij}\tau}, \qquad J_i^-(\omega_{ij})=\int_0^\infty d\tau\langle f_i(q,0)f_i(q,\tau)\rangle e^{-i\omega_{ij}\tau}, \tag{7g}$$

where

$$f_i(q,\tau)=e^{iH_B\tau}f_i(q,0)e^{-iH_B\tau}.$$

In our treatment, the bath is stochastic, thus we replace the quantum mechanical correlation functions appearing in Eq. (7g) with their time-symmetrized classical analogs.[11] In terms of the classical correlation functions, the spectral densities become

$$J_i^+(\omega_{ij})=(1+e^{\beta\hbar\omega_{ij}})^{-1}\times\int_0^\infty d\tau\langle f_i(q,\tau)f_i(q,0)\rangle_{\rm cl}e^{-i\omega_{ij}\tau}, \qquad J_i^-(\omega_{ij})=(1+e^{-\beta\hbar\omega_{ij}})^{-1}\times\int_0^\infty d\tau\langle f_i(q,0)f_i(q,\tau)\rangle_{\rm cl}e^{-i\omega_{ij}\tau}. \tag{8}$$

Using these definitions for the spectral densities, it is easy to verify that the population relaxation rates obey the detailed balance relation, i.e., $(R_{ii,jj}/R_{jj,ii})=e^{\beta\hbar\omega_{ij}}$.

To construct the Redfield tensor, we assume the bath correlation functions decay exponentially with a correlation time, τ_c. Assuming this time is much shorter than any timescale relevant to the system allows us to make the replacement $J_i(\omega)\rightarrow J_i(0)=\langle f_i^2\rangle\tau_c$. The spectral densities that enter into the Redfield tensor thus have the form

$$J_i^+(\omega_{ij})=f_i^2\tau_c(1+e^{\beta\hbar\omega_{ij}})^{-1}, \qquad J_i^-(\omega_{ij})=f_i^2\tau_c(1+e^{-\beta\hbar\omega_{ij}})^{-1}. \tag{9}$$

We begin by examining the role of coherence transfer terms in the relaxation of an oscillator in which the coupling to the bath contains only the linear term. Thus in this example, interactions that lead to pure dephasing between any pair of levels are absent. The primary observables of interest are the system energy and the value of the coordinate, Q. The average values of these observables are given by

$$\langle E(t)\rangle=\mathrm{Tr}\{\rho(t)H_s\}, \tag{10}$$

$$\langle Q(t)\rangle=\mathrm{Tr}\{\rho(t)Q\}. \tag{11}$$

The density matrix at $t=0$ is given by the superposition state

$$\rho_{66}(0)=\rho_{77}(0)=\rho_{67}(0)=\rho_{76}(0)=0.5, \qquad \rho_{ij}(0)=0; \quad i,j\neq 6,7,$$

which corresponds to a coherence between levels 6 and 7. The linear coupling term, $f_1^2\tau_c$, is chosen such that $T_1(1\rightarrow 0)=2.0$ ps. Note from the form of the one-phonon relaxation terms that the population relaxation rate increases linearly with quantum number. Thus $T_1(n\rightarrow n-1)=n^{-1}T_1(1\rightarrow 0)$. Since we are working in the eigenstate representation, the system energy depends only on the diagonal elements of the system density matrix. The only terms of the Redfield tensor that enter into the relaxation of the energy are the one-phonon population relaxation terms. The decay of the system energy to its equilibrium value is shown in Fig. 1(a). The decay fits well to a single exponential with a time constant, τ_E, of 4.2 ps.

The coherence present in the density matrix at $t=0$ results in an initial value for the ensemble-averaged coordi-

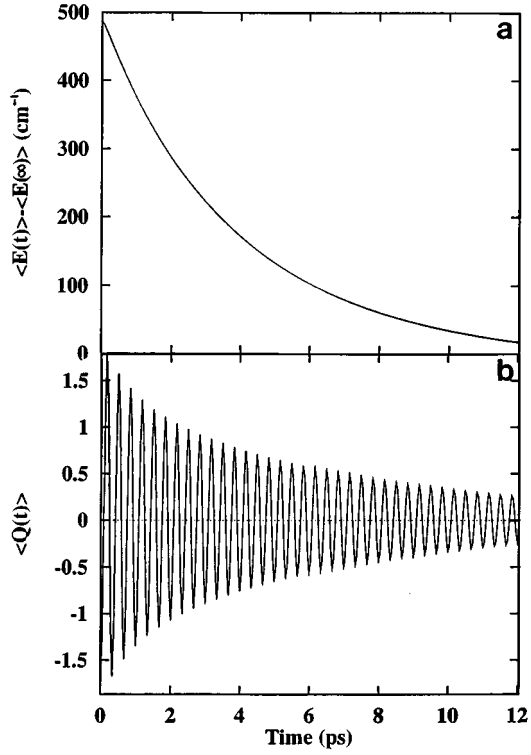

FIG. 1. (a) Decay of the nonequilibrium energy for a quantum oscillator. The equilibrium energy in the system is given by $\langle E(\infty)\rangle=[\hbar\omega/\exp(\hbar\omega/kT)-1]$. $\omega/2\pi=100\ \mathrm{cm}^{-1}$, $T_1(1\rightarrow 0)=2.0$ ps, $T_2^*(\Delta n=1)=\infty$, $T=298$ K. (b) Decay of the coordinate amplitude obtained using the full Redfield tensor.

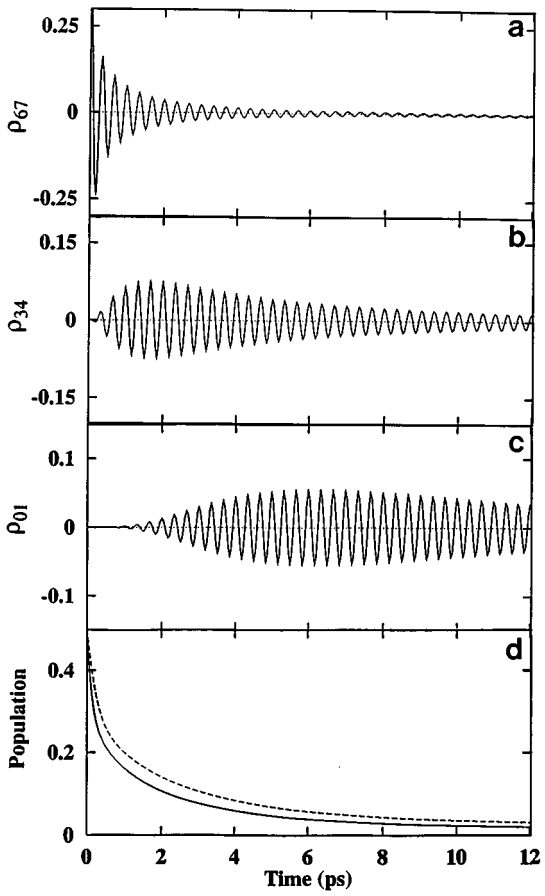

FIG. 2. Time-dependence of selected density matrix elements for the oscillator described in Fig. 1 obtained using the full Redfield tensor. (a) $\rho_{67}(=\langle 6|\rho|7\rangle)$; (b) ρ_{34}; (c) ρ_{01}; (d) (---) ρ_{66};(—)ρ_{77}.

nate, $\langle Q\rangle$, that is displaced from its equilibrium value of zero. The dissipative dynamics are governed primarily by the one-phonon population relaxation terms and the one-phonon coherence transfer terms. The decay of the amplitude is shown in Fig. 1(b). Fitting the data to the function $\langle Q(t)\rangle=\langle Q(0)\rangle\cos(\omega t)e^{-t/\tau_Q}$ yields a value of 6.2 ps for τ_Q. We thus have the unusual condition that the loss of energy from the system to the environment occurs faster than the destruction of phase coherence in the system, i.e., $\tau_E<\tau_Q$, which is the multilevel analog of $T_1<T_2$. The origin of the above result can be seen by examining the effect of the coherence transfer terms on the dynamics. Since the average value of the coordinate depends only on the off-diagonal density matrix elements, we look at the magnitudes of these elements as a function of time. The magnitudes of the coherence for several pairs of levels are shown in Figs. 2(a)–2(c). We see a rapid destruction of the initial phase coherence involving levels $n=6$ and $n=7$. The only dephasing terms here are the one-phonon relaxation terms which are quite large at such high energies. The temporal behavior of the off-diagonal elements shows that as the population relaxes to lower levels, phase coherence is also transferred. The efficiency of the coherence transfer process is a result of the harmonic form of the potential, which guarantees exact frequency matching between pairs of levels that differ by the same number of quanta. An anharmonic form of the potential would result in frequency mismatches rendering the coherence transfer terms less effective; however, if the T_1 processes are fast compared to $\omega_{i-1}^{-1}-\omega_i^{-1}$ in such a system, coherence transfer terms should still play an important role.

The above result clearly shows that if one equates the energy relaxation time of the oscillator with T_1 and the damping time of the coordinate with the dephasing time, T_2, the relation between these two times does not necessarily obey the Bloch relation, Eq. (1c). We next ask whether the relation between T_1 and T_2 hold for a pair of levels in a multilevel system when coherence transfer processes are operable. Figure 2(d) shows the decay of population in $n=6$ and $n=7$ as a function of time employing the same initial condition and linear coupling parameter as stated above. The lifetimes for the levels are given by $T_1(n=6)=R_{66,66}^{-1}=0.19$ ps and $T_1(n=7)=R_{77,77}^{-1}=0.16$ ps. The coherence between these two levels is shown in Fig. 2(a). Two things are clear form the decay profiles; (i) the decays are nonexponential, which results from the fact that the population of a given level is determined by several competing source and loss terms, and (ii) the dephasing rate of the coherence is smaller than one-half the sum of the two population decay rates. Thus in multilevel systems the dynamics of any given level receive contributions from relaxation tensor elements neglected at the Bloch level. The appropriate Redfield tensor elements, however, do obey the Bloch relation, i.e.,

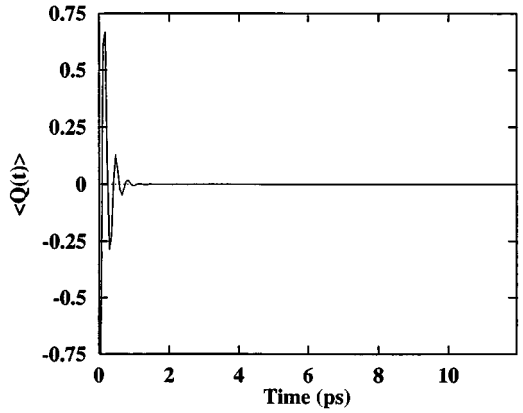

FIG. 3. Decay of the coordinate amplitude for a quantum oscillator obtained using the Bloch approximation. $\omega/2\pi=100$ cm^{-1}, $T_1(1\rightarrow 0)=2.0$ ps, $T_2^*(\Delta n = 1) = \infty$, $T=298$ K.

$$R_{67,67}=\frac{1}{T_2}=\frac{1}{T_2^*}+\frac{1}{2}\left(\frac{1}{T_{1,n=6}}+\frac{1}{T_{1,n=7}}\right)$$

as shown in Eq. (7d).

We contrast the behavior seen above with that obtained on the identical system employing a multilevel Bloch approximation. Here the only terms included in the Redfield tensor are the one-phonon population relaxation, $R_{ii,jj}$, and dephasing, $R_{ij,ij}$, terms. The decay of the coordinate amplitude is shown in Fig. 3. The energy relaxation dynamics are unaffected by the absence of non-Bloch relaxation terms since only population relaxation terms enter into the dynamics. However, the coordinate relaxes on a subpicosecond time scale due to the rapid loss of population. The absence of coherence transfer terms traps the coherence to those levels initially populated. In this case, we have the usual inequality $\tau_E > \tau_Q$.

It is interesting to investigate the situation where the coupling of the oscillator to the bath contains both linear and quadratic terms. This introduces pure dephasing as well as two-phonon relaxation terms. An interesting competition now arises between the pure dephasing and two-phonon population relaxation terms, which increase the rate of dephasing, and the two-phonon coherence transfer terms which lead to more efficient transfer of coherence to pairs of levels at lower energy. Figure 4 shows results for a system with $T_1(1\rightarrow 0)=2.0$ ps and $T_2^* = 6.0$ ps. Though the linear coupling term is the same as that in the earlier example, the τ_E time is now reduced 1.8 ps due to the presence of two-phonon relaxation pathways. The decay of the coordinate amplitude occurs on a similar time scale, which shows that even in the presence of pure dephasing mechanisms, the observation of vibrational oscillations does not imply that energy relaxation is slower than the coordinate damping time.

The results above clearly demonstrate the pitfalls of applying the Bloch equations to the dynamics of a multilevel system and point out the importance of coherence transfer terms in determining the relation between the dephasing and energy relaxation times. These results are significant in light of the recent results on iodine recombination following solvent caging at low temperature by Apkarian and co-workers.[6] They observe coherent oscillations of the newly reformed I_2 molecule out to 4 ps, though energy relaxation is found to be largely complete on a subpicosecond time scale. The apparent efficiency of coherence transfer processes in this system may be a result of a near harmonic form for the I_2 potential function in the presence of the krypton cage. This would give rise to transfer of phase between pairs of levels with nearly identical transition frequencies.

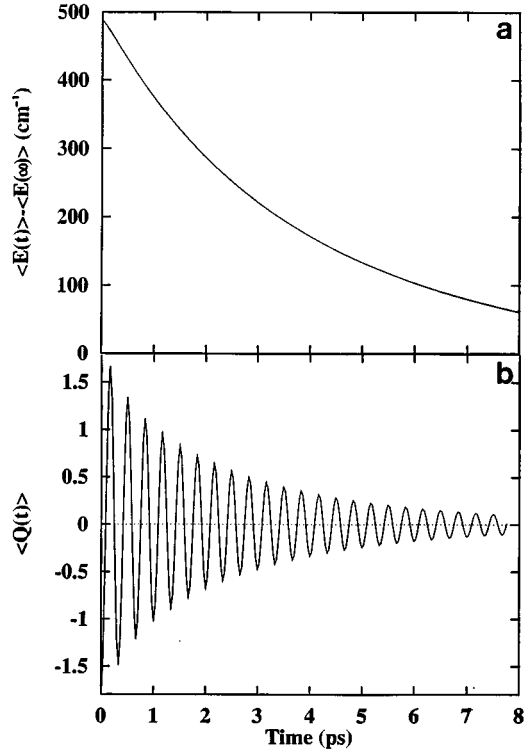

FIG. 4. (a) Decay of the nonequilibrium energy for a quantum oscillator in the presence of pure dephasing. $\omega/2\pi=100$ cm^{-1}, $T_1(1\rightarrow 0)=2.0$ ps. $T_2^*(\Delta n=1)=6.0$ ps, $T=298$ K. (b). Decay of the coordinate amplitude obtained using the full Redfield tensor.

IV. TWO ELECTRONIC STATES COUPLED TO A QUANTUM OSCILLATOR

The second model we discuss pertains to the quantum dynamics of nonadiabatic transitions in a dissipative medium. The effect of dissipation on condensed phase curve crossing phenomena has been treated by numerous workers employing both quantum mechanical[8,9,12–23] and semiclassical descriptions.[24–28] We consider two electronically excited states coupled to a quantum harmonic oscillator, which, in turn, is weakly coupled to a thermal bath. This serves as a simple model for condensed phase photoinduced curve crossing processes where the electronic states couple strongly to a single nuclear mode such as a low frequency protein phonon or an underdamped solvent librational mode. We have recently examined in detail the competition between vibrational energy relaxation and dephasing and electron tunneling in this system[8,9] and the manner in which this competition is manifested in time-resolved fluorescence

measurements.[9] In this section, we will be concerned with understanding the influence of vibrational coherence on the dynamics of curve crossing and the conditions under which a curve crossing process can lead to vibrationally coherent product formation. The motivation for our studies comes from the recent observations of vibrational coherence in time-resolved studies of the primary electron transfer step in bacterial photosynthesis[1,2] and vibrationally coherent all *trans*-retinal formed by ultrafast isomerization of 11-*cis* retinal in the rhodopsin system.[3]

The Hamiltonian for our model system is

$$H_S = H_G + H_E, \tag{12}$$

with

$$H_G = |G\rangle\left\{a^+a + \frac{1}{2}\right\}\hbar\omega\langle G|,$$

$$H_E = |1\rangle\left[\epsilon_1 + \left(a^+a + \frac{1}{2}\right)\hbar\omega + g_1(a+a^+)\right]\langle 1| + |2\rangle$$
$$\times\left[\epsilon_2 + \left(a^+a + \frac{1}{2}\right)\hbar\omega + g_2(a+a^+)\right]\langle 2|$$
$$+ J\{|1\rangle\langle 2| + |2\rangle\langle 1|\},$$

where G refers to the ground electronic state and 1,2 refer to excited electronic states. The system coordinate is denoted by Q and the bath coordinates by q. ω is the vibrational frequency and a and a^+ are the boson operators for the system coordinate, which is defined such that $Q=0$ corresponds to the minimum of the ground state surface. The tunneling interaction between diabatic states $|1\rangle$ and $|2\rangle$ is denoted by J. The electron–phonon couplings, g_i, have units of energy and are related to the excited state dimensionless displacements, Δ_i, by $g_i = -\Delta_i\hbar\omega/\sqrt{2}$ and ϵ_i is the vertical energy separation between the ground state and excited state i.

As in the previous section, the system–bath interaction for diabatic state $|i\rangle$ is assumed weak and expanded to second order in the system coordinate about the minimum,

$$V_i(\mathbf{q},Q) = f_1^{(i)}(\mathbf{q})(Q-\Delta_i) + f_2^{(i)}(\mathbf{q})(Q-\Delta_i)^2. \tag{13}$$

Vibrational energy relaxation, dephasing, and coherence transfer rates in a given diabatic state can be constructed from matrix elements of V as shown in the previous section.

Convenient implementation of Redfield theory requires that we work in the representation which diagonalizes the system Hamiltonian. In this representation, the only coupling present is the weak coupling between the system levels and the thermal bath. The details of our approach derive from earlier work of Wertheimer and Friesner[29] and Wertheimer and Silbey[30] and are discussed in Refs. 8 and 9. Briefly, the procedure is as follows. The system Hamiltonian operator and system–bath coupling operator are set up in the diabatic representation. Denoting the matrix that transforms between the diabatic and eigenstate representations as U, we make the following transformations:

$$E = U^+ H_E U,$$

$$\Psi = U^+ V U, \tag{14}$$

$$\rho = U^+ p U,$$

where E is the diagonal matrix of system energies, and p (ρ) is the density matrix in the diabatic (eigenstate) representation. Ψ contains the matrix elements of the system–bath coupling operator in the eigenstate representation. In this representation, the Redfield equations become

$$\dot{\rho}_{NM}(t) = -i[(E_N - E_M)/\hbar]\rho_{NM} - \sum_{PQ} R_{NM,PQ}\rho_{PQ}(t) \tag{15}$$

with

$$R_{NM,PQ} = -\frac{1}{\hbar^2}\int_0^\infty d\tau\Big[\langle\Psi_{QM}(0)\Psi_{NP}(\tau)\rangle e^{-i\omega_{QM}\tau}$$
$$+\langle\Psi_{QM}(\tau)\Psi_{NP}(0)\rangle e^{-i\omega_{NP}\tau}$$
$$-\delta_{QM}\sum_S\langle\Psi_{NS}(\tau)\Psi_{SP}(0)\rangle e^{-i\omega_{SP}\tau}$$
$$-\delta_{PN}\sum_S\langle\Psi_{QS}(0)\Psi_{SM}(\tau)\rangle e^{-i\omega_{QS}\tau}\Big],$$

where N,M,P,Q label eigenstates of the system. As before, we replace the spectral densities in Eq. (15) by their values at $\omega=0$. Numerical solution of the Redfield equations provide us with the time-dependent density matrix in the eigenstate representation. The total population in a given diabatic state is then found by transforming back to the diabatic representation and tracing over all vibronic levels belonging to that diabatic state. Thus the population of state $|i\rangle$ is given by

$$P_i(t) = \mathrm{Tr}_i[p(t)]. \tag{16}$$

While population dynamics provide insight into coherence effects on the dynamics of electronic curve crossing, additional information pertaining to coherent vibrational motion can be obtained from the ensemble-averaged system coordinate

$$\langle Q(t)\rangle = \mathrm{Tr}[p(t)Q], \tag{17}$$

where the coordinate operator is defined (in the diabatic representation) as

$$\hat{Q} = |1\rangle\left[\frac{1}{\sqrt{2}}(a+a^+ + \Delta_1)\right]\langle 1| + |2\rangle\left[\frac{1}{\sqrt{2}}(a+a^+ + \Delta_2)\right]\langle 2|$$
$$= \hat{Q}_1 + \hat{Q}_2. \tag{18}$$

The average value of this operator is influenced by both vibrational coherences and electronic population dynamics. Defining the coordinate operator in the manner above allows us to separate the contributions to $\langle Q(t)\rangle$ from vibrationally coherent reactant and product motion.

The initial density matrix, ρ_0, in our simulations is generated by solving the equation of motion to second order in the system–field interaction, $H_{\mathrm{SF}} = -\mu\cdot E(t)$, where $E(t)$ is the electric field of the laser pulse, assuming (1) only state $|1\rangle$ is "bright," and (2) there is no dissipation during the pulse.[9] If the displacement of this state from the ground state is zero, then the effect of the optical excitation is to "lift" the thermal distribution of the ground state up to the excited state. If

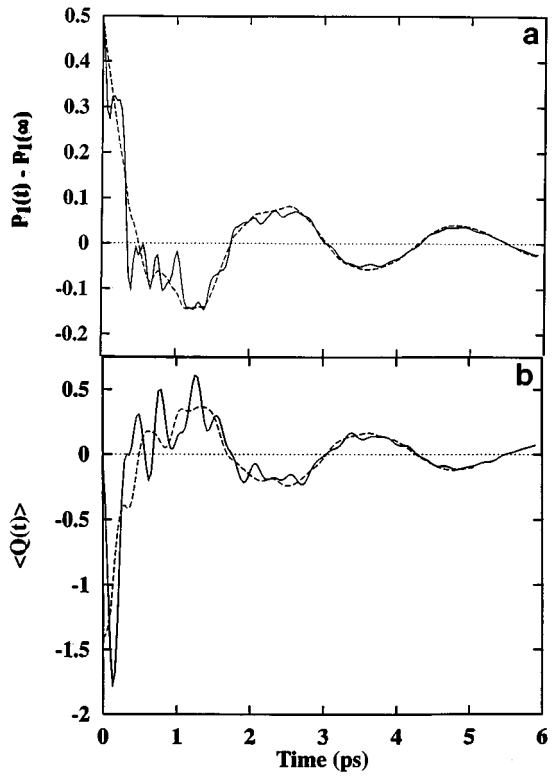

FIG. 5. Quantum dynamics of the symmetric double well potential with $\omega/2\pi$=100 cm^{-1}, J=50 cm^{-1}, $T_1(1\rightarrow0)$=2.8 ps, $T_2^*(\Delta n = 1)$ = 6.0 ps, T=298 K. (—) coherent preparation; (---) thermal preparation. (a) Nonequilibrium population in the initially prepared electronic state. (b) Reaction coordinate trajectory. The crossing of the diabatic surfaces occurs at Q=0.

the ground and ''bright'' states have different potential minima, however, the excitation process results in a localized vibrational wavepacket on the upper surface providing the pulse is short compared to the vibrational period (i.e., impulsive). Our main objective here is to determine the influence of the initial state on the subsequent dynamical behavior, thus we focus on the dynamics of curve crossing following impulsive excitation both with and without excited state displacement.

In the examples that follow, the system–bath coupling terms are chosen such that the relaxation times of the diabatic vibrational states are $T_1(1\rightarrow0)$=2.8 ps and $T_2^*(n,n-1)$ = 6.0 ps. The vibrational frequency is $\nu=\omega/2\pi$=100 cm^{-1}. The electron–phonon couplings are chosen such that g_2-g_1=200 cm^{-1} corresponding to a dimensionless displacement of $\Delta=\Delta_2-\Delta_1$=2.82, and the temperature is 298 K. The excitation pulse has a center frequency of $\omega_L-\omega_{0\text{-}0}$=500 cm^{-1} with a temporal duration of 20 fs.

As a first example, we compare the effect of the preparation of the initial state on the curve crossing dynamics in a symmetric double well potential in which the bare tunneling matrix element is one-half the vibrational frequency. Figure 5(a) shows the nonequilibrium population dynamics of the initially excited state for the case where $\Delta_1=-\Delta_2=-1.41$ and for the case where $\Delta_1=0$ and $\Delta_2=2.82$. In the former case, the impulsive excitation results in the formation of a vibrational coherence involving several Franck–Condon active levels. In the latter case, the preparation results in a thermal density matrix in the initial state. The crossing of the diabatic surfaces in this case occurs at $Q=0$. The time scale of the tunneling interaction is comparable to the dephasing time scale, thus we observe pronounced electronic recurrences in both cases. The lower frequency modulation, with a period of 2–2.5 ps results from the transfer of population between pairs of levels that are resonant. For example, the effective electronic coupling for the $0\rightarrow0$ transition is given by $J_{0\text{-}0}=J\langle0|0\rangle=J\exp(-S)$=6.85 cm^{-1}, where $S=1/2\ \Delta^2$ is the Huang–Rhys factor. The period associated with this coupling is $(2J_{0\text{-}0})^{-1}$=2.42 ps. The $1\rightarrow1$ transition has an effective coupling of $J_{1\text{-}1}$=20 cm^{-1}, which has a period of 0.83 ps. In the case of coherent preparation of the initial state, modulation at higher frequencies is observed, which is a result of vibrational phase interference effects between different Franck–Condon transitions. This is evident from the population dynamics for the case of thermal preparation. The modulation at the higher frequency is absent, whereas quantum beats are still observed at the lower frequency.

Further insight into the role of quantum coherences on the curve crossing process can be obtained from the ensemble-averaged value of the system coordinate. Figure 5(b) shows the reaction coordinate trajectory for both coherent and thermal preparation. In the former case, it is clear that the vibrational coherence created initially persists through the curve crossing process. For the case of thermal preparation, the initial value of the coordinate corresponds to the minimum of the potential surface of state $|1\rangle$. As the system moves through the crossing region, weak oscillations become apparent. The period of these oscillations is shorter than that associated with any of the effective electronic couplings between resonant levels and thus correspond to coherences between levels involving different numbers of vibrational quanta.

The relative importance of various coherences in the curve crossing dynamics can be seen in the frequency domain. Figure 6 shows Fourier transforms of the population decays and the coordinate trajectories shown in Fig. 5. The Fourier transforms of the population dynamics for both the thermally prepared and coherently prepared cases are dominated by components corresponding to coupling between diabatic states with the same number of vibrational quanta, i.e., $J_{0\text{-}0}$ and $J_{1\text{-}1}$. In addition to the components corresponding to coupling between resonant diabatic states, we also pick up higher frequency components. This is evident from the inset in Fig. 6(a), which shows an expanded view of the highfrequency region. These frequencies are larger than any of the resonant coupling terms involving states initially populated and correspond to coherences between eigenstates that have large projections onto diabatic states with different number of vibrational quanta. The appreciable mixing of nonresonant diabatic states results from the bare electronic coupling and diabatic vibrational frequency being of comparable magnitude. In the case where the initial state is vibrationally coherent, the higher frequency components are much more pronounced; however, the same components appear in the case where the preparation of the bright state is thermal.

Similar results are seen in the Fourier transforms of the

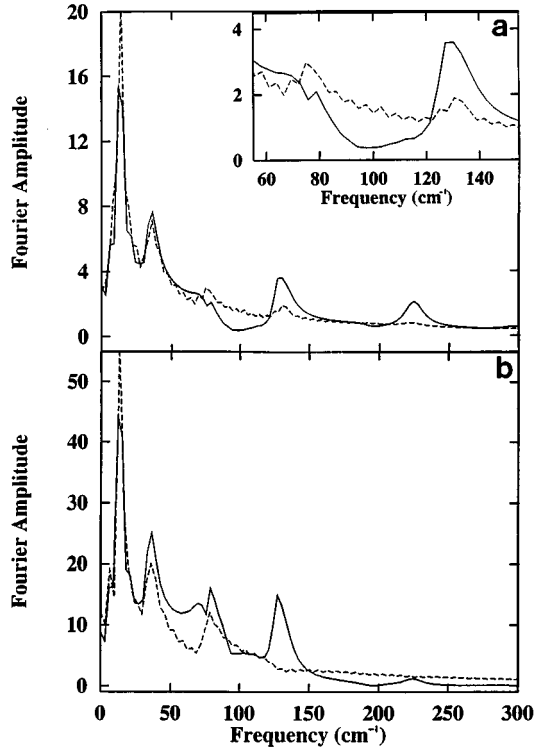

FIG. 6. (a) Magnitude of the Fourier coefficients obtained from the Fourier transform of the population dynamics shown in Fig. 5(a). Inset, expanded view of the region near the diabatic vibrational frequency. (b) Magnitude of the Fourier coefficients obtained from the Fourier transform of the system coordinate dynamics shown in Fig. 5(b). (—) coherent preparation; (---) thermal preparation. The Fourier amplitude is defined as $A(\omega)=\{|\int_0^\infty dt e^{-i\omega t}F(t)|^2\}^{1/2}$.

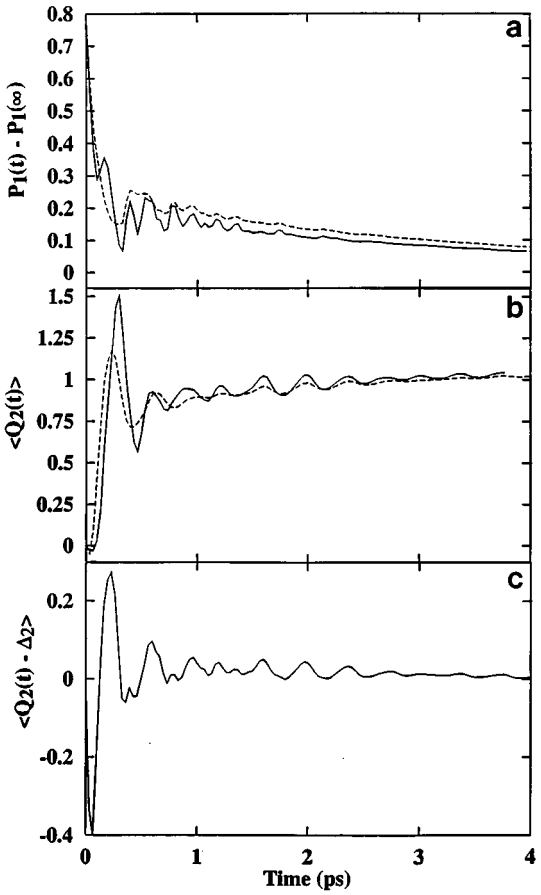

FIG. 7. Quantum dynamics of the asymmetric double well potential with $\Delta\epsilon=300$ cm^{-1}, $\omega/2\pi=100$ cm^{-1}, $J=50$ cm^{-1}, $T_1(1\rightarrow0)=2.8$ ps, $T_2^*(\Delta n=1)=6.0$ ps, $T=298$ K. (—) coherent preparation; (---) thermal preparation. (a) Nonequilibrium population of the initially prepared electronic state. (b) Product coordinate trajectory, $\langle Q_2(t)\rangle$. (c) Vibrational contribution to the product coordinate, $\langle Q_2(t)-\Delta_2\rangle$. The crossing of the diabatic surfaces occurs at $Q=-1.10$.

reaction coordinate trajectories. Note that in this symmetric model there is no component in the coordinate trajectory that corresponds to the diabatic vibrational frequency. This is not surprising given that each diabatic state is strongly mixed with a resonant state by the electronic interaction. When viewed from the diabatic representation, the appearance of frequency components that correspond to coherences between states with different number of vibrational quanta denotes vibrationally coherent motion. It is clear from the above results that even in the case where the time scale associated with the electronic coupling is somewhat longer than the unperturbed vibrational period, the product state is formed vibrationally coherent even when no such coherence exists in the initially prepared state.

Also apparent from the above example is that the strong electronic coupling necessary to generate a vibrationally coherent product from a thermally prepared initial state leads to numerous electronic recurrences. We next ask if there are circumstances under which an irreversible curve crossing process from a thermally prepared state can lead to a coherently vibrating product. Intuitively, we expect this to most likely occur when the electronic coupling is such that population of product vibrational levels occurs on a timescale comparable to or faster than one-half the vibrational frequency and the dephasing of coherences between reactant and product levels is fast compared to the electronic recurrence time. The latter situation will occur if the system is biased so that the product is created with considerable excess vibrational energy. The population relaxation rates increase with vibrational quantum number, thus rapid relaxation out of the crossing region would occur in such a system. Figure 7(a) compares the population dynamics for an asymmetric double well with $J=100$ cm^{-1} and $\Delta\epsilon=300$ cm^{-1} under conditions of coherent and thermal preparation. The displacement of the two surfaces is identical to that of the previous model. The population decay in both cases is dominated by a fast ($\sim$100 fs) component and a slower (picosecond) component that shows weak modulation, which is effectively damped out by 1.8 ps. The corresponding product coordinate trajectories, $\langle Q_2(t)\rangle$, are shown in Fig. 7(b). The energy bias in this model is such that the crossing of the diabatic surfaces occurs at $Q=-1.10$, which means the system is near the activationless region. It is clear in both cases that the product is formed vibrationally coherent with quantum beats observable out to times well past the time at which quantum beats are observed in the population dynamics.

As mentioned earlier, the average value of the coordinate contains contributions from coherences between vibrational

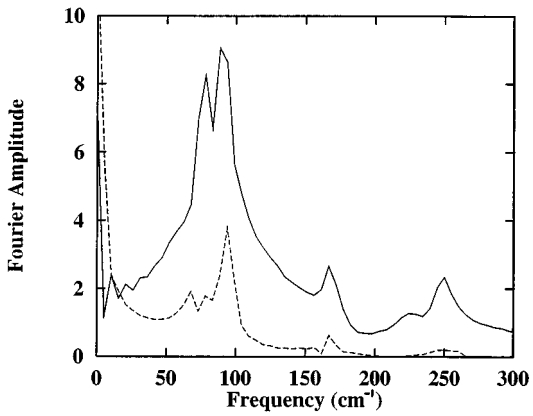

FIG. 8. Magnitude of the Fourier coefficients obtained form the Fourier transform of product coordinate dynamics shown in Fig. 7(c). (—) Fourier transform of full trajectory (0–4 ps). (---) Fourier transform of truncated trajectory (1.8–4 ps).

levels within a diabatic state and from electronic population dynamics. In the asymmetric system described above, the splitting of the diabatic surfaces due to the tunneling interaction is larger than the diabatic vibrational frequency. This gives rise to strong mixing of diabatic states near the crossing region with the lowest-lying states being essentially diabatic in character due to the energy bias. Note that even though the site states are harmonic, the first three spacings in the eigenstates of the product well are 96, 91, and 77 cm^{-1}, respectively. Unlike the earlier example with smaller electronic splitting, the distinction between electronic coherence effects and vibrational coherences is not so clear. To focus on the purely vibrational coherence, we must subtract out that contribution to $\langle Q_2(t)\rangle$ that comes from transfer of population between wells. This can be done by calculating $\langle Q_2(t)-\Delta_2\rangle$ [see Eq. (18)], which is shown in Fig. 7(c). This average value depends only on the off-diagonal elements of the density matrix for state $|2\rangle$ in the diabatic representation, and thus provides a measure of the magnitude of the product vibrational coherence. The Fourier transform of $\langle Q_2(t)-\Delta_2\rangle$ is shown in Fig. 8. Fourier components appear over a wide range of frequencies reflecting the complex spectrum of eigenvalues due to the strong electronic mixing; however, again, we see no appreciable amplitude at the diabatic vibrational frequency (i.e., 100 cm^{-1}). This result seems surprising given that at energies corresponding to the bottom of the product well the eigenstates are nearly pure product diabatic states due to the energy bias. If coherence transfer terms are operable, then we expect vibrational relaxation of the product will result in the appearance of coherences that oscillate at nearly the diabatic frequency. Further analysis of the data in Fig. 7(c) shows that this is indeed the case. Note that the observed beat pattern is complex at short times ($<$1.8 ps) becoming more regular at longer times. The Fourier transform of $\langle Q_2(t)-\Delta_2\rangle$ at times greater than 1.8 ps is also shown in Fig. 8. Here we clearly see a component at $\sim$96 cm^{-1}, which corresponds to the energy gap between the two lowest lying eigenstates, which are essentially the $n=0$ and $n=1$ diabatic levels of the product. This component is not present in the short time data and grows in as a result of coherence transfer processes. This result clearly shows that straightforward Fourier analysis of experimental decays in systems systems undergoing electronic curve crossing can lead to erroneous conclusions regarding diabatic vibrational frequencies.

V. CONCLUDING REMARKS

The single well calculations show that the often-made assumption that observation of oscillatory contributions to pump–probe or fluorescence data imply slow vibrational energy relaxation may not be generally supportable. Coherence transfer terms, neglected at the optical Bloch level, are responsible for this effect. Interestingly, the presence of pure dephasing does not destroy the coherence transfer since the concommitant two-phonon relaxation process enhances energy relaxation. Anharmonicity will reduce the degree of coherence that can be transferred down a well, but as the double well results show (see below) is not likely to remove the effect entirely.

In the two state calculations, coherence transfer also plays a critical role in producing coherent motion in final state levels well below the crossing region. Without this effect, coherences at frequencies corresponding to unperturbed vibrations of the product would not be observed. The deviation from harmonicity in the product well due to the electronic coupling does not preclude the appearance of coherent motion in the 0-1 superposition state following relaxation. At this point it is appropriately to recall that our calculations involved a single internal degree of freedom. In real molecules it is possible that ''spectator'' modes that are orthogonal to the reaction coordinate will be impulsively excited and may transfer their coherence to the product. In this case beat frequencies at site state frequencies will appear immediately the product is formed, rather than requiring relaxation out of the crossing region. Perhaps this will allow discrimination between reaction coordinate and other degrees of freedom.

In our calculations, we have not attempted to model the experimental signals for specific systems; however, we note that for a monotonic difference potential, the wavelength of absorption corresponds to a particular internuclear distance,[3,4,31] thus the ensemble-averaged value of Q_2 and the signal obtained in a time-resolved absorption experiment are directly connected. Recently, several experimental studies have detected vibrational coherences in products formed as a result of electronic curve crossing. For example, Wang *et al.*[3] have shown that the isomerization of 11 *cis*-retinal leads to vibrationally coherent all-*trans* retinal as determined by the wavelength-dependence of the phase of the oscillations seen in the transient absorption of the product. It is interesting to ask what types of coherences are being measured in this type of experiment. Is one measuring $\langle Q_2(t)\rangle$, which, as stated earlier, contains contributions from both electronic population dynamics and vibrational coherences, or $\langle Q_2(t)-\Delta_2\rangle$, which contains only vibrational information? The answer to this would seem to depend on whether the reactant and product are spectrally distinct. If this is the case, then coherent cycling of the population between wells will contribute to the signal. If the transient absorption spectra of reactant and

product have substantial overlap, then oscillations in the transient absorption (or emission) decay would provide direct observation of vibrational coherence.

ACKNOWLEDGMENTS

G.R.F. acknowledges support from the NSF. We would like to thank David Jonas, Ralph Jimenez, Steven Bradforth, Jeffrey Cina, and Larry Bretthorst for helpful discussions.

[1] M. H. Vos, F. Rappaport, J.-C. Lambry, J. Breton, and J.-L. Martin, Nature **363**, 320 (1993).
[2] R. J. Stanley and S. G. Boxer, J. Phys. Chem. **99**, 859 (1995).
[3] Q. Wang, R. W. Schoenlein, L. A. Peteanu, R. A. Mathies, and C. V. Shank, Science **266**, 422 (1994).
[4] N. F. Scherer, D. M. Jonas, and G. R. Fleming, J. Chem. Phys. **99**, 153 (1993).
[5] K. Wynne, C. Galli, and R. M. Hochstrasser, J. Chem. Phys. **100**, 4797 (1994).
[6] R. Zadoyan, Z. Li, C. C. Masters, and V. A. Apkarian, J. Chem. Phys. **101**, 6648 (1994).
[7] A. G. Redfield, Adv. Magn. Reson. **1**, 1 (1965).
[8] J. M. Jean, R. A. Friesner, and G. R. Fleming, J. Chem. Phys. **96**, 5927 (1992).
[9] J. M. Jean, J. Chem. Phys. **101**, 10 464 (1994).
[10] A. M. Walsh and R. D. Coalson, Chem. Phys. Lett. **198**, 293 (1992).
[11] D. W. Oxtoby, Adv. Chem. Phys. **47**, 487 (1981).
[12] A. Matro and J. A. Cina, J. Phys. Chem. **99**, 2568 (1995).
[13] W. T. Pollard and R. A. Friesner, J. Chem. Phys. **100**, 5054 (1994).
[14] R. D. Coalson, D. G. Evans, and A. Nitzan, J. Chem. Phys. **100**, 437 (1994).
[15] R. Schneider, W. Domcke, and H. Koppel, J. Chem. Phys. **92**, 1045 (1989).
[16] Y. Tanimura and S. Mukamel, J. Chem. Phys. **101**, 3049 (1994).
[17] A. J. Leggett, S. Chakravarty, A. T. Dorsey, M. P. A. Fisher, A. Garg, and W. Zwerger, Rev. Mod. Phys. **59**, 1 (1987).
[18] A. Garg, J. N. Onuchic, and V. Ambegoakar, J. Chem. Phys. **83**, 4491 (1985).
[19] M. Morillo, D. Y. Yang, and R. I. Cukier, J. Chem. Phys. **90**, 5711 (1989).
[20] P. Parris and R. Silbey, J. Chem. Phys. **83**, 5619 (1985).
[21] J. N. Onuchic and P. G. Wolynes, J. Phys. Chem. **92**, 6495 (1988).
[22] M. Topaler and N. Makri, J. Chem. Phys. **101**, 7500 (1994).
[23] O. Kuhn, V. May, and M. Schreiber, J. Chem. Phys. **101**, 10 404 (1994).
[24] P. G. Wolynes, J. Chem. Phys. **86**, 1957 (1987).
[25] J. E. Straub and B. J. Berne, J. Chem. Phys. **87**, 6111 (1987).
[26] R. E. Cline and P. G. Wolynes, J. Chem. Phys. **86**, 3836 (1987).
[27] A. Warshel and J.-K. Hwang, J. Chem. Phys. **84**, 4938 (1986).
[28] W. Wang, K. A. Nelson, L. Xiao, and D. F. Coker, J. Chem. Phys. **101**, 9663 (1994).
[29] R. Wertheimer and R. A. Friesner, Proc. Natl. Acad. Sci. **79**, 2138 (1982).
[30] R. Wertheimer and R. Silbey, J. Chem. Phys. **74**, 686 (1981).
[31] R. B. Bernstein and A. H. Zewail, J. Chem. Phys. **90**, 829 (1989).